Appendix E-1

Geometrical Model of the Cutting Process

  The target planes (the desired planes after cutting) were defined by a minimal set of three independent variables (t, β, and γ) in a geometrical reference frame (R_0) with a reference plane (A) (Fig. E-1). The variable t represents the height of the target plane measured in millimeters along the Z axis of R_0. The variable β represents the depth angle measured in degrees in the YZ plane of R_0. The variable γ represents the front angle measured in degrees in the XZ plane of R_0 that corresponds to the front face of the simulated bones during the cuts. To obtain a large range of depth and front angles, we constructed three target planes with the following values for t, β, and γ, respectively: Plane 1 (25, 30, and 10), Plane 2 (30, 10, and −20), and Plane 3 (45, −20, and 20). Plane 1 and Plane 2 have positive depth angles while Plane 3 has a negative depth angle. Practically, the operators had to position their wrist in substantial ulnar deviation to perform the cuts of Plane 3.

  To evaluate the cutting error, we defined two parameters, flatness (F) and location (L), in accordance with the ISO1101:2004 standard[33]. F represents the form of the cut plane and is defined as the minimum distance in millimeters between two parallel planes that include the cut plane (Fig. E-2). L refers to the position of the cut plane with respect to the target plane (Fig. E-2). L is defined as half the distance in millimeters between two planes that present the following properties: they are parallel to the target plane, they are positioned at an equal distance from the target plane, and they include the cut plane. Previous experiments[34] have demonstrated the relevance of L in gathering all information about translational and rotational errors in the independent variables t, β, and γ.

Evaluation of the Cutting Process

  To evaluate the cutting errors, we first digitized the cut planes with a precision of 1 µm using a coordinate measuring machine (SIGNUM SL; Mycrona, Elgin, Illinois) with a spherical sensor (2 mm in diameter). The cut-plane digitization was performed according to the guidelines for an ISO-based evaluation of macroscopic properties such as location and flatness[43]: the 2-mm diameter of the spherical sensor enabled us to neglect microscopic properties such as roughness. The initial cut-plane data set consisted of a matrix of 10 × 10 measurement points, consisting of a squared distribution on the cut section of the simulated bone and acquired in the z-direction of R_0 with the zero reference considered to be the reference plane A (Fig. E-2). We then fitted this coordinate set to a least square plane, a common procedure in checking ISO parameters[43].

  The cutting errors were calculated with use of numerical computation software (MATLAB; The MathWorks, Natick, Massachusetts). The error e_t was calculated as the distance along the Z axis of R_0 between the least square plane and the target plane. The error e_β was calculated as the angular difference in the YZ plane of R_0 between the normals of the least square plane and the target plane. The error e_γ was calculated as the angular difference in the XZ plane of R_0 between the normals of the least square plane and the target plane. Because the three target planes covered a large range of depth and

front angles, we also calculated the rotational errors in terms of their absolute values ($e_{|\beta|}$, $e_{|\gamma|}$).

To determine the parameter F, we calculated the maximum and minimum distances (f_{max} and f_{min}), normal to the least square plane, between the measured points and the least square plane; F was then calculated as the sum of the absolute values of f_{max} and f_{min}. The parameter L was calculated as the absolute value of the maximum distance, normal to the target plane, between the measured points and the target plane.

Process 1: Freehand Cutting

A series of seventy-two cuts was performed with use of the freehand cutting process. Six operators (Operators 1 through 6), experienced in bone cutting, each performed twelve cuts, four cuts in each of the three target planes, alternating among Plane 1, Plane 2, and Plane 3. For the freehand process, the operators cut the simulated bones without the use of jigs and guides. We allowed the operators to palpate the simulated bones before the cuts to introduce them to the bone anatomy. We then covered the surgical site with a blue drape that had holes to simulate realistic conditions (Fig. E-3) (for example, in periacetabular surgery[9,44] and ankle surgery[12]). Our goal was to limit the (lateral) visibility and accessibility to the bone and also to prevent the operators from defining geometrical landmarks on the precision vises or the rectangular geometry of the simulated bones (which would have been an unrealistic and irrelevant action). To provide an estimate of the depth and front angles, a printed sheet with a graduated angular scale from 0° to 30° in 5° increments was given to the operators. Finally, the entry point of the target planes was marked with a pencil on the surface of the simulated bone starting from reference plane A, while the exit point was hidden by the blue drape.

Process 2: Navigated Freehand Cutting

A series of seventy-two cuts was performed with the aid of a navigation system (Surgetics; Praxim, Grenoble, France) by the same operators (Operators 1 through 6) using the same cutting sequence as employed in Process 1. A computed tomography scan (made with a spiral Elscint Twin CT Medical Scanner [ElsMed, Holon, Israel]) of the simulated bone was made with 0.4-mm x-y resolution and a 1.1-mm slice thickness with a 0.7-mm step in the z-direction. The navigation system can handle slice thicknesses of 1 to 3 mm. We constructed a three-dimensional model of the simulated bone by using reconstruction and segmentation algorithms provided by the navigation system. To minimize the modeling error of the simulated bone, we constructed the three target planes by defining the independent variables (t, β, and γ) starting from reference plane A (the bottom face of the polyurethane block, corresponding to the bottom face of the three-dimensional model), as described in Figure E-1.

The navigated freehand process was designed to provide operators with visual feedback of the position and orientation of the saw blade with respect to the simulated bone (Fig. E-4). The navigation system employed the spine module that enables the planning and navigation of intrapedicular screw insertions. We adapted this module for direct navigation of the saw blade around the simulated bone. The main geometrical dimensions of the blade were included in the system, and the oscillation plane of the blade was calibrated with use of the calibration unit. Finally, we registered the simulated bone with the three-dimensional computed tomography model using paired-point and

surface-based algorithms provided by the navigation system. This registration step was performed only once before the navigated cuts were performed, since our experimental test bed allowed us to fix the simulated bones at exactly the same position. After registration, we checked its accuracy by sensoring a set of ten points on each face of the simulated bone. We calculated the distances between these points and the three-dimensional bone model with the measuring tool of the navigation system. These distances were always smaller than 0.5 mm; this is within the accuracy of the localizer (Polaris; NDI, Waterloo, Ontario, Canada), which has an accuracy of 0.5 mm and 0.5° according to the manufacturer.

A dynamic reference basis was rigidly fixed to the bone-clamping device. The dynamic reference basis and the oscillating saw were equipped with patterns of infrared reflecting markers. The Polaris localizer tracked these patterns with an accuracy of 0.5 mm and 0.5°. Using the tracking information, we were able to calculate the position and orientation of the saw blade with respect to the reference frame R_0 attached to the simulated bone. The operators performed the cuts using the free mode of the navigation system with real-time visual feedback of the cut on a monitor screen.

Process 3: Robot-Assisted Cutting

A series of twelve cuts was performed with use of an industrial six-axis robot (Viper s650; Adept Technology, Livermore, California). According to the manufacturer, the robot has an XYZ positioning repeatability of ±0.03 mm. The internal calibration of the robot (originally performed by the manufacturer) was verified, as described by Khalil and Dombre[45]. Geometrically simple motions of the end-effector, such as linear and circular segments, were defined into the work volume of the application and programmed into the robot controller. An external optical localizer (MicronTracker Hx40; Claron Technology, Toronto, Ontario, Canada) tracked the position and the orientation of the end-effector equipped with a black-and-white marker, with an accuracy of 0.5 mm and 0.5°. We then verified that the robot performed the desired motions within the accuracy of the localizer.

The robotic process was designed for fully automated cutting. The robot and the bone-clamping device were mounted on the same worktable. The oscillating saw was rigidly attached to the wrist of the robot (Fig. E-5). The MicronTracker localizer was used to sensor both the faces of the simulated bone and the end-effector of the robot by using a tracking pointer marked with a black-and-white pattern.

Starting from the points of the simulated bone sensored by the MicronTracker localizer, we constructed the bone model and the reference frame R_0, as described in Figure E-1, by fitting the faces XY (reference plane A), YZ, and XZ of the simulated bone to a least square plane. We then constructed the target planes by defining the three independent variables (*t*, β, and γ) starting from the reference plane A. After that, we checked the accuracy of the registration between the simulated bone and the bone modeled in the robot controller by sensoring a set of ten points on each face of the simulated bone. We calculated the distances between these points and the three-dimensional bone model. These distances were always smaller than 0.5 mm; this is also within the accuracy of the MicronTracker localizer.

Finally, starting from the points sensored on the end-effector of the robot and knowing the kinematic parameters of the robot, we calculated the position of the robot

base with respect to the simulated bone and calibrated the position and orientation of the saw blade in the reference frame R_0.

We programmed the robot controller with a cutting-process algorithm to move the oscillating saw blade along the target planes. To bypass the absolute positioning error of an industrial six-axis robot (typically induced by gravity, and of an order of magnitude of a few millimeters), we developed our cutting-process algorithm to control the robot motions relative to the initial calibrated position of the saw blade in the reference frame R_0, as described by Khalil and Dombre[45]. An operator (Operator 1) used a handheld terminal to control normal starting and stopping procedures and emergency stops. The robot translation speed was set at 10 mm/s.

Appendix E-2

Discussion About the Error in the Cut-Plane Height

The error in the cut-plane height was subject to significant variations (Fig. 2, *A*). With the robot-assisted process, the error was significantly decreased compared with that associated with the purely freehand and navigated freehand processes. However, the error associated with the navigated cutting was larger than that observed with the freehand process. We can discuss these results by presenting three major considerations:

1. Cutting bones with an oscillating saw with a 1.4-mm-thick blade produced a kerf of an order of 2 mm (Fig. 1). The kerf was measured on the twelve cuts of the robot-assisted process. We did not account for this kerf during the evaluation of the cutting processes. Therefore, we can reasonably expect a negative bias equal to half a kerf (about 1 mm) on the calculated errors of the cut-plane height and location (Fig. 2, *A* and *D*). By definition, this kerf has no influence on the rotational errors or the flatness (Fig. 2, *B* and *C*). As a consequence, accounting for the kerf in the discussion, the translational error encountered when positioning the oscillating saw was about 0.1 mm for the robot, 0.9 mm for the operators assisted by the navigation system, and 0.3 mm for the operators working freehand.

2. Cutting bones with an oscillating saw with a 100-mm-long blade produced some flexure of the blade. We did not account for this deformation in the navigation system. We visually noted a flexure of the blade induced by the operator, just before the cutting, when he placed the saw in contact with the simulated bone to position the blade according to the visual feedback provided by the system. The flexure was not present in the robot-assisted process because the robot motions were programmed into the controller, and it was not present in the freehand process because the entry point of the target plane was marked on the surface of the simulated bone.

3. We favored the freehand cutting process by marking the entry point of the target plane on the surface of the simulated bone, while the exit point was hidden by the blue drape with holes. Marking the entry point with a pencil on the bone surface simulated a surgical reality: before performing freehand bone-cutting, surgeons can use a marker to place some landmarks on the skin in order to guide the cutting[12,14]. In our study design, we decided to mark the entry point beforehand in order to prevent the operators from defining landmarks on the precision vises or the simple rectangular bone geometry, which would have been an unrealistic and irrelevant action. For the robot-assisted process, the entry point was automatically virtually defined in the robot controller by

defining the independent variables (t, β, and γ) in the constructed reference frame R_0. For the navigated freehand process, the entry point had to be reached by positioning the oscillating saw on the bone surface according to the visual feedback provided by the system. However, even if the freehand cutting process was favored, the results first revealed a relatively small 0.9-mm error for the navigated positioning of the saw (Fig. 2, *A*) and secondly demonstrated that location was nevertheless significantly improved by the navigation system (Fig. 2, *D*).

As a conclusion about the cut-plane height, we think that both accounting for kerf during the tool calibration step and correcting for blade flexure during the cuts (for example, by measuring the forces applied to the blade) are two potential solutions for improving the global translational error.
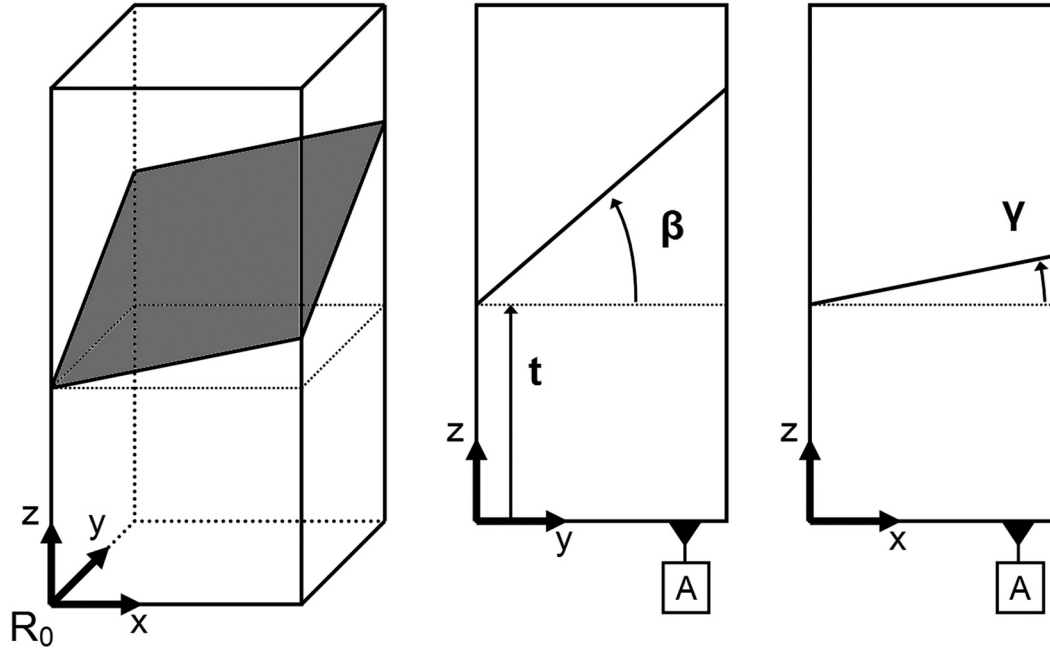
Fig. E-1

Geometrical model of the cutting process. The target plane (the gray plane in the three-dimensional view) is defined in a reference frame R_0 by a set of three independent variables: height (t) in millimeters, depth angle (β) in degrees, and front angle (γ) in degrees. A = the reference plane for the definition of t, β, and γ.
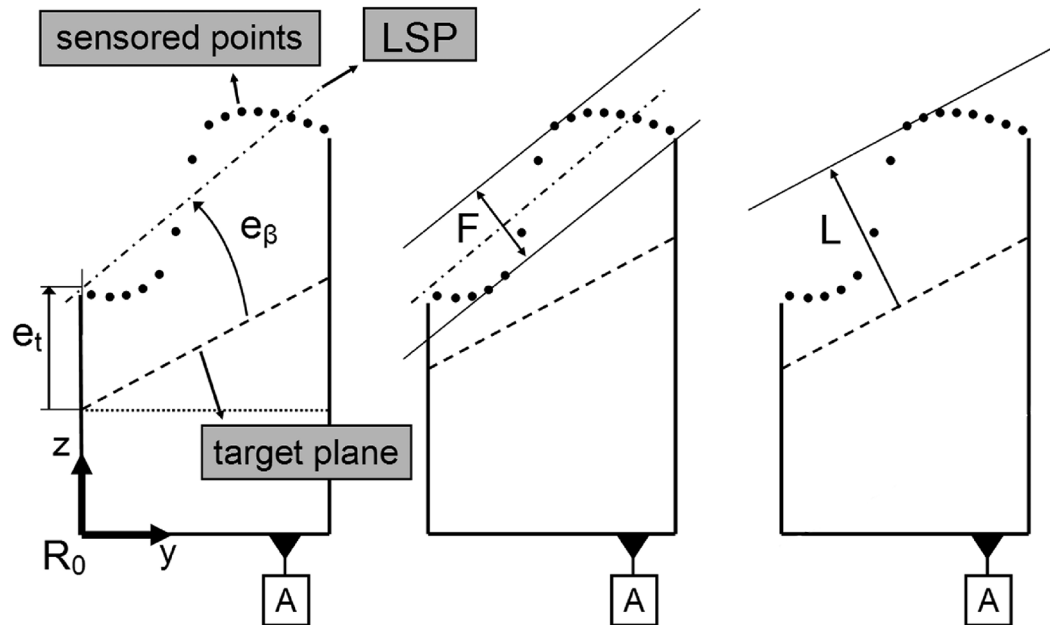

Fig. E-2

Definition of the cutting errors: error in the height (e_t) in millimeters, error in the depth angle (e_β) in degrees, flatness (F) in millimeters, and location (L) in millimeters. The target plane is the dashed line. The cut plane is sampled by the measurement points (the sensored points). The measurement points are fit to a least square plane (LSP). A (the bottom face of the block in the left panel) = the reference plane for the definition of t, β, and γ.
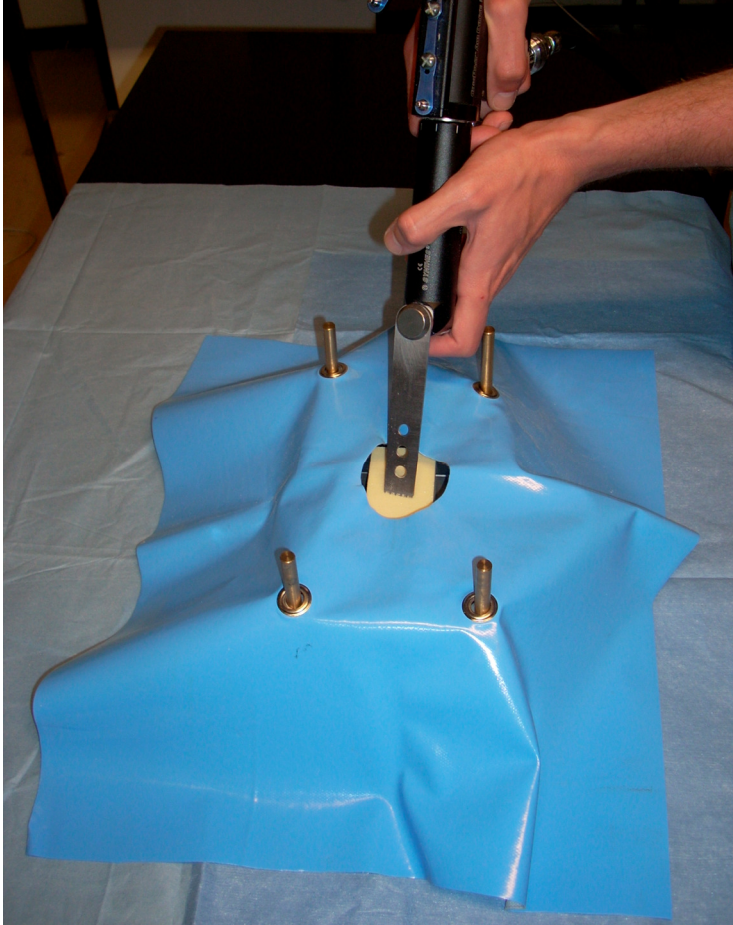
Fig. E-3
The freehand cutting process with no available jigs. A blue drape with holes covered the
simulated bone to prevent the operators from defining geometrical landmarks on the
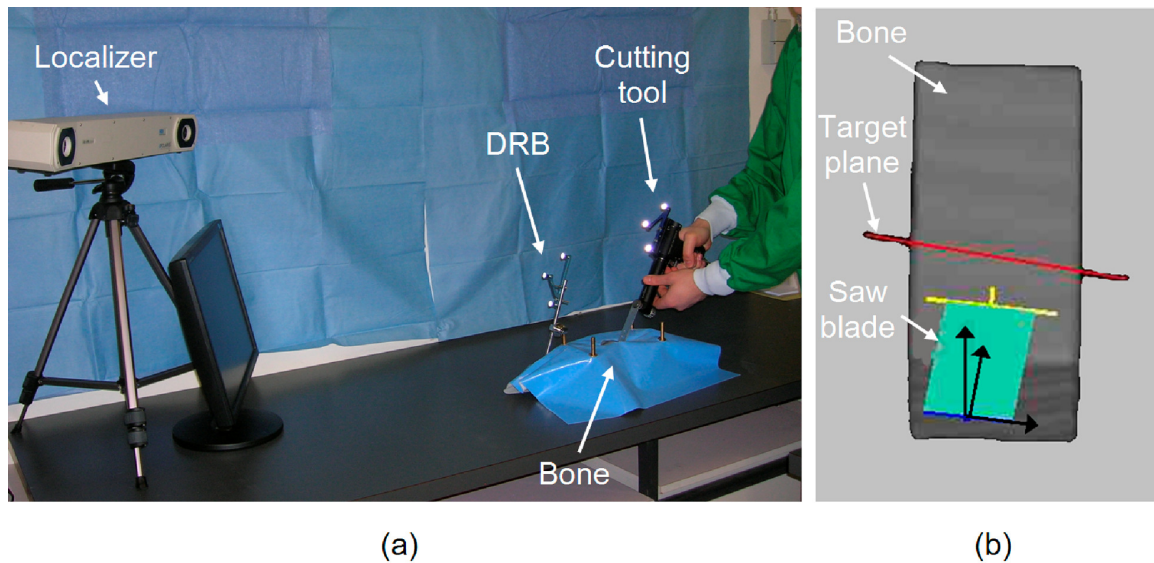precision vises or the rectangular geometry of the simulated bones.

(a)   (b)

Fig. E-4
a: The navigated freehand cutting process with no available jigs. A dynamic reference
basis (DRB) is fixed to the simulated bone. The oscillating saw is tracked in real time by
an optical localizer. *b:* The real-time visual feedback consists of a virtual three-
dimensional model of the simulated bone. The target plane is represented by a red line.
The position and orientation of the saw blade are continuously refreshed. The oscillation
plane of the blade is represented by a green rectangle delimited by a yellow line (the
distal extremity of the blade) and a blue line (the proximal extremity of the blade). The
blade is correctly aligned on the target plane when the red, yellow, and blue lines
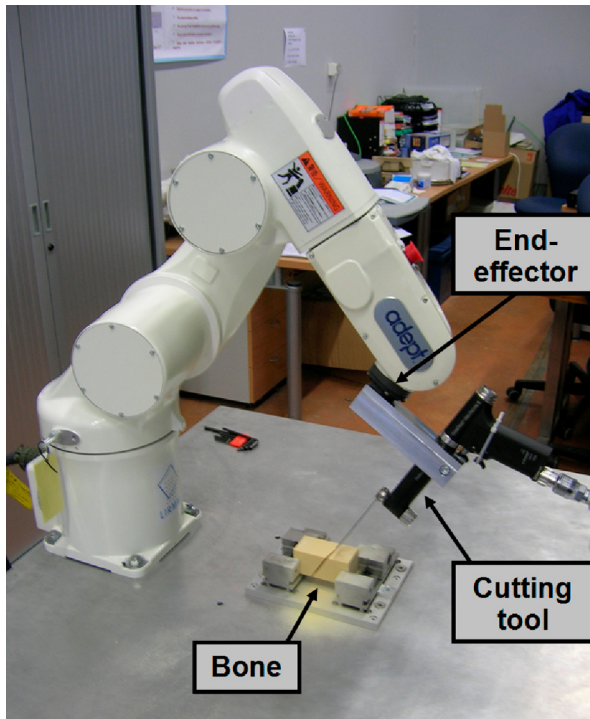overlap.

Fig. E-5
The robot-assisted cutting process. The oscillating saw is rigidly attached to the end-effector of the robot. The simulated bone and the saw blade were previously registered and calibrated by using an external optical localizer. The robot controlled the position and orientation of the saw blade in the reference frame R_0 (defined in Fig. E-1).